Deep Neuro-Fuzzy System For Early-Stage Identification of Parkinson's Disease Using SPECT Images

Jothi S¹, Anita S^{2*}, Sivakumar S³

¹Department of Computer Science, Jayaraj Annapackiam College for Women, Theni, 625601, Tamilnadu, India

²Department of Electronics and Communication Engineering, St. Anne's College of Engineering and Technology, Panruti, 607 106, Tamilnadu, India

³Department of Computer Science, Cardamom Planters' Association College, M. K. University, Madurai, 625 513, Tamilnadu, India

E-mail: srjothics@annejac.ac.in, sranitaa@stannescet.ac.in, sivakumar s@cpacollege.org

*Corresponding author

Keywords: Parkinson's disease, volume containing DaTSCAN image slices, deep neuro-fuzzy system genetic algorithm, particle swarm optimization

Received: May 5, 2025

A neurodegenerative disorder called Parkinson's disease (PD) is identified at the increasing loss of neurons that produce dopamine in the substantia nigra region of human brain. It significantly impairs motor and non-motor functions, thereby diminishing the overall quality of life in affected individuals. A novel framework is proposed for detecting early stage of PD, employing Deep Neuro-Fuzzy System (DNFS) optimized with Particle Swarm Optimization (PSO) and Genetic Algorithm (GA). Data utilized for this analysis are extracted from 16 image slices showing striatal uptake content in the striatum, named as volume-containing DaTscan image slices (VCDIS) taken from the database called Parkinson's Progression Markers Initiative (PPMI). The shape and texture characteristics of segmented VCDIS are utilized as features which are combined with Striatal biding ratio (SBR) to distinguish Healthy Individuals (HI) from early-stage PD (EPD). The dataset includes values of 620 DaTscan images with SBR values: 430 from EPD cases and 190 from HI. The effectiveness of the framework is evaluated using 70:30 and 80:20 split ratios, based on metrics such as accuracy, loss, F1 score, precision, and recall. The DNFS-PSO model is presented an impressive accuracy of 98.77% and an error rate of 0.0199 for the chosen features using a 70:30 data split. The outcomes of the proposed model potentially aid clinicians in prompt diagnosis.

Povzetek: Za zgodnje odkrivanje Parkinsonove bolezni iz SPECT (DaTSCAN) je uveden globoki sistem (DNFS), ki združi CNN-izbor značilk in fuzzy-pravila, optimizirana s PSO in GA, na 16-slojnih VCDIS (PPMI). Značilke: oblika/tekstura + SBR.

1 Introduction

Parkinson's Disease (PD) is an advanced neurological disorder impairing the central nervous system (CNS) at the degeneration of dopaminergic neurons within substantia nigra in the midbrain. It leads to a considerable reduction or complete depletion of dopamine, a neurotransmitter essential to regulate motor control and coordinate communication between the brain and the limbs. PD is generally recognized as a age-related disorder, with an estimated global prevalence of approximately 1% among individuals over the age of 55 [1-4].

Motor and non-motor symptoms are the clinical indicators to identify PD. Tremors, shuffled gait, stooped posture, Freezing of Gait (FoG), dysphonia, and bradykinesia are categorized as the primary motor symptoms. Whereas anosmia affecting the sense of smell, fatigue, disrupted sleep patterns, fluctuations in body weight, alterations in mood and cognitive function, coronary artery

complications, as well as digestive tract problems are non-motor symptoms which become apparent only in the later stages. As these symptoms are not found in the early stage of individuals, detecting PD in its early stage (EPD) is exceptionally challenging [5]. To address this, a novel and resourceful approach is required to discriminate between HI and EPD [6-8], and being done using Single Photon Emission Computed Tomography (SPECT) images which are known as DaTscan images [8].

DaTscan image slices are employed to quantitatively measure dopamine transporter levels in putamen and caudate regions of the brain, providing a comprehensive assessment. Traditionally, trained radiologists have performed standard examination for assessing DaTscan images. These images are taken from Parkinson's Progression Markers Initiative (PPMI) database. The database is an international and multicenter database that tracks the disease, its progression and conducts regular assessments of patients to identify new biomarkers that

assist experts in diagnosing the disease [9]. Thus, these images significantly help in identifying EPD.

The methods of identifying EPD with the help of SPECT images initially rely on Visual Inspection (VI) of the striatum's appearance. This approach is time-consuming and lacked reliability, with experts often differing in their observations, leading to variability in both individual and collective findings. VI offers around 5% of false rate in diagnosing DaT scan Images [10]. Efforts to enhance disease identification are accelerated by extracting features from a 2D slice and subsequently from averaged image slices that achieves 97% of accuracy [11]. Later, changes in DaT content and striatum shape during the early stages are monitored through investigation of 3D images consist of 91 slices [12]. However, the complexity of 3D image investigation received limited attention from clinical practitioners, prompting the necessity of simpler and more accurate technique for EPD identification.

Anita et al. [13] suggested a simplified model to address the above said diagnostic challenges, utilizing 12 image slices of a SPECT image as a single slice and records 98.23% of classification accuracy. However, this method falls short in effectively diagnosing EPD, as it leaves several slices that are essential for capturing the complete shape and structure of the striatum. Hence, a novel approach is introduced recognizing a set of sixteen slices (slices 34 to 49) as a 2D slice (2D) that capture the entire shape of the striatum to enhance the diagnostic accuracy and model simplicity.

Furthermore, image processing techniques, including preprocessing, segmentation, and feature extraction, have significantly aided to the clinical experts in disease diagnosis. The extracted features are utilized to identify neural disorders by categorizing individuals using Machine Learning (ML) algorithms. Though, the performance of ML algorithms like Extreme Learning Machine (ELM), Support Vector Machine (SVM) and Artificial Neural Network (ANN) offers appreciable results, it is greatly influenced by the presence of redundant and irrelevant features in the dataset, leads to over-fitting issues. To enhance the performance, it is essential to eliminate these unnecessary attributes and choose optimal subsets of features which in turn reduces the over fitting issues. Hence, the hybrid intelligence algorithm called Deep neural fuzzy system (DNFS) [14] has been proposed to learn the deep relationships between the features for the first time in diagnosing EPD.

DNFS, a part of Artificial Intelligence (AI), integrates the adaptive learning capabilities of Deep Neural Networks (DNNs) with the reasoning power of Fuzzy system addressing challenges particularly in handling nonlinear, imprecise and high dimensional data [15,16]. Its effectiveness extends in the realm of medical image analysis and classification [17]. Aversano developed a deep learning model hybridization with a fuzzy layer that process the data from various feet sensors of PD patients. The fuzzy layer aids in managing uncertainty and imprecision in the sensor data and offers the classification accuracy of 85.83% due to presence of more parameters [18]. To enhance diagnostic accuracy, a CNN is applied to shape, texture features, and SBR for optimal feature

selection. Additionally, the fuzzy system generates rules, which are further optimized using PSO and GA.

Here are the key contributions of the proposed model.

- 1. An innovative method for the early identification of PD with the help of SPECT images is presented. Out of 91 slices in each SPECT image, only the 16 image slices (34 to 49) exhibit a rich striatal uptake content. Therefore, those image slices are specifically selected to enhance the diagnostic accuracy [13] as they provide a comprehensive analysis of the striatum's shape. Consequently, the substantial performance in recognizing EPD is achieved utilizing biomarkers like SBR values, shape and texture attributes of VCDIS.
- 2. The DNFS is applied for the first time to diagnose early PD which utilizes shape, texture features and SBR values as inputs for the framework. However, the traditional frameworks encounter challenges related to predefined rule sets in fuzzy system (FS) and fixed model size in Convolutional neural networks (CNN). To address these challenges, the DNFS integrates a Convolutional Neural Network (CNN) with a Fuzzy System (FS) in a dynamic framework. In this architecture, the CNN selects the most prominent features, the Fuzzy System formulates the rule sets, depending on the nature of the input data.
- 3. Particle swarm optimization (PSO) and Genetic algorithm (GA) are used by Deep neuro fuzzy system for optimizing dynamic fuzzy rules that ensures effective and relevant rule alone in learning process. These optimized rules are performing a significant role in diagnosing EPD by reducing redundant data and conflicting fuzzy rules. By deriving the most effective fuzzy rule sets through GA and PSO, the system aims to minimize classification errors and support early, accurate diagnosis of PD.

The following sections are systematized as: Section 2 offers operational workflow of this novel model, accompanied by a diagrammatic representation. Also delve into the preprocessing, segmentation, and feature extraction algorithms employed, as well as introduce the DNFS, PSO and GA algorithms utilized in the framework. Section 3 discusses the results and comparative analyses. Finally, Section 4, offers conclusions.

2 Methodology overview

The proposed system's procedural workflow, as depicted in Figure 1, involves the extraction of features such as shape and texture features, that include area, entropy, mean, correlation, and sharpness estimation from VCDIS. Additionally, Striatal Binding Ratio (SBR) values from different brain regions-Putamen_R (Pu_R), Caudate_R (Ca_R), Putamen_L (Pu_L), and Caudate_L (Ca_L)-are combined with shape and texture features to form the complete feature set. CNN selects the most important

features from this set. The FS then frames rules based on the input data, and these rules are optimized using Particle Swarm Optimization (PSO) and Genetic Algorithm (GA) to improve classification accuracy.

2.1 Study cohort in detail

Diagnosis of EPD relies on the analysis of VCDIS and the calculation of SBR values. The image slices and SBR values are obtained from PPMI database. It contains SPECT images categorized into two groups: Early Parkinson's Disease (EPD) and Healthy Individuals (HIs), as determined by expert evaluation [11]. In total, 620 images are collected for research purposes, with 190 from HIs and 430 from EPD patients. EPD patients are selected based on a mean ±standard deviation of Hohen and Yahr

stage (H&Y) of 1.50 ± 0.50 (criteria 1 and 2 of Hoehn and Yahr Scale)

The reliability and consistency of the images in the database are ensured as they were preprocessed. The preprocessing steps include iterative image reconstruction to enhance the robustness of the images. Subsequently, the images' anatomical alignment is made standardized through the application of spatial normalization and attenuation correction [19]. As a result of these preprocessing steps, the processed images have dimensions of 91x109x91 cubic voxels, each with a width of 2mm, following the DICOM format. To calculate the SBR values, the slices with the highest uptake regions are averaged and following formula is used.

$$SBR = \left(\frac{Pu_L L + Ca_L + Pu_R + Ca_R}{\text{occipital region}}\right) - 1 \tag{1}$$

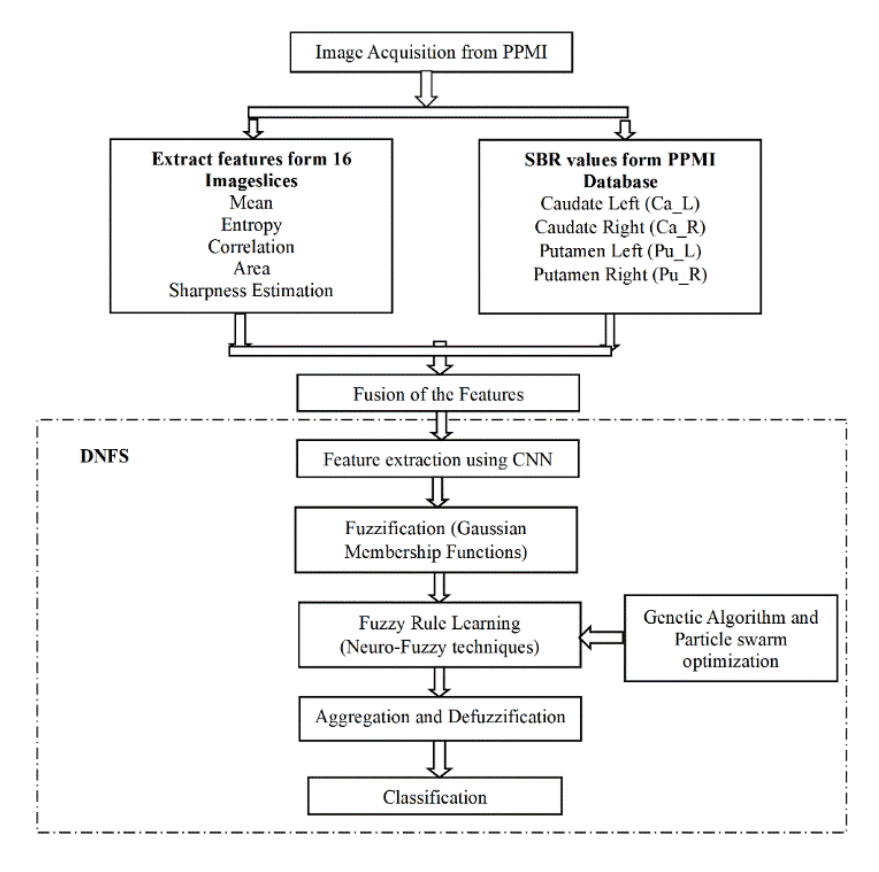


Figure 1: Operational sequence of Deep Neuro-Fuzzy system

2.2 Selection procedure for rich striatal uptake image slices

DaTscan or SPECT images are acquired when a drug (radiopharmaceutical) binds specifically to the dopamine transporters in the brain. Each captured DaTscan image contains ninety-one slices, ranging from the bottommost to the top of the brain as shown in Figure 2. Among these slices, only few are relevant for identifying PD. Those most significant slices are alone selected for the investigation of the present work that exhibit high specific uptake content. The remaining slices, where striatal uptake content gradually diminished to nearly imperceptible levels are omitted.

This approach aligns with the guidelines set forth by the Society of Nuclear Medicine (SNM) [20] and enhances the ability to identify the presence of disease. Building upon the recommendations of SNM, Prashanth et al. [21] specifically averaged slices numbered from 34 to 49 and identified them as having high striatal uptake. Subsequently, Anita et al. further refined this selection by selecting 12 slices as a single 2D slice from this range to develop an accurate diagnostic system for EPD. To improve upon this prior system, proposed system has chosen 16 slices, as showed in Figure 3. These 16 image slices provide valuable three-dimensional information derived from 2D image slices, offering a simpler yet more effective technique compared to the 12 VRIS [13]. Since

EPD has a direct impact on the size of the striatum, the proposed work opted for VCDIS because they maintain the continuity of the striatum's shape.

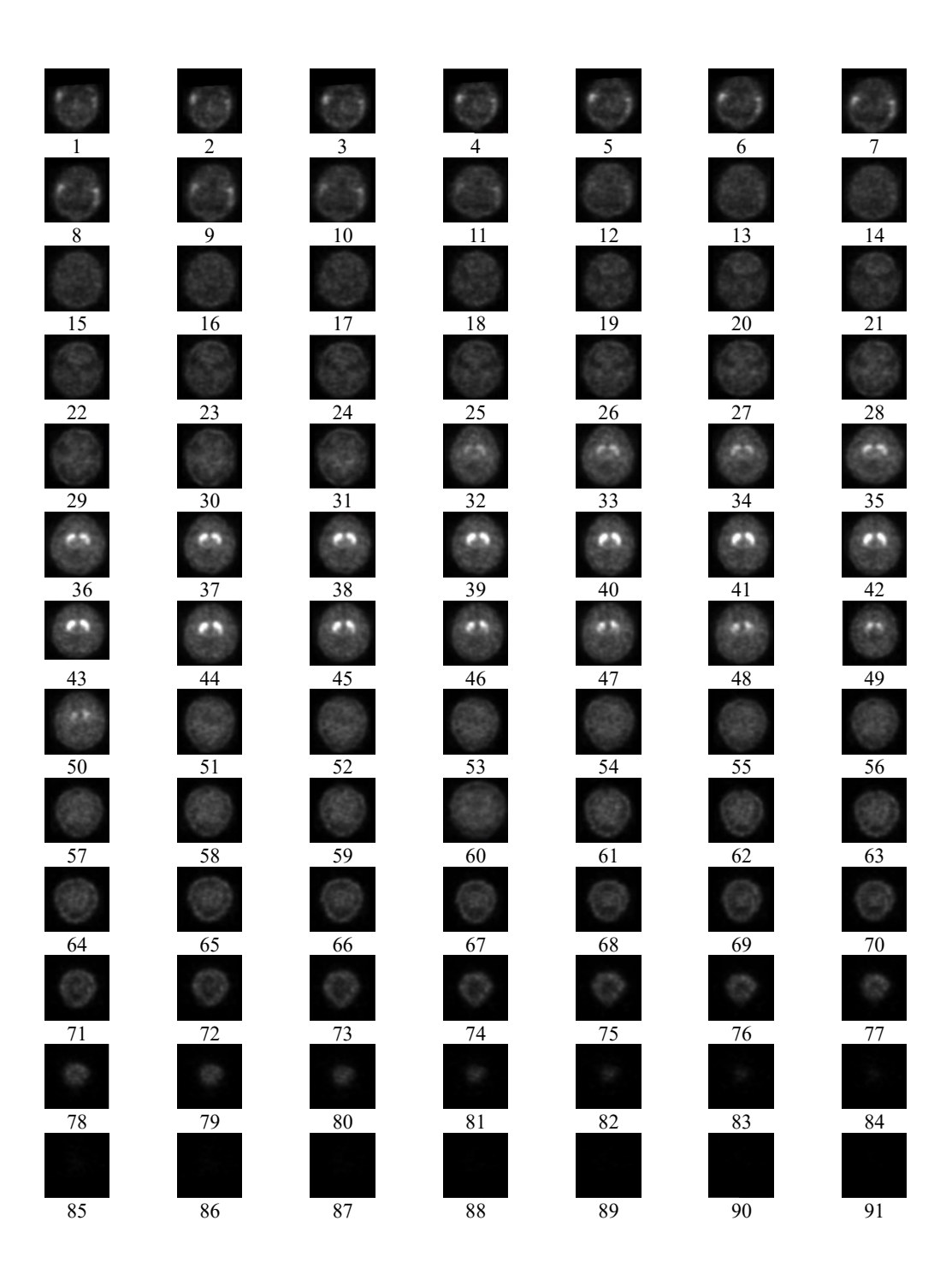


Figure 2: Ninety-one SPECT Image Slices of HI

2.3 Image Preprocessing and segmentation

The preprocessing method utilized here is a bilateral filter, which aims to enhance the striatum's appearance while simultaneously improving its edge definition. The filter achieves this by calculating the combined weights of neighbouring pixels. The intensity of the pixels and their spatial distance from one another are used to calculate these weights. This filter effectively retains the image's

boundaries by taking into account the average noise in neighbouring pixels. The mathematical expression that characterizes this filter's behavior at a given input pixel location, denoted as 'x,' can be described as follows

$$I(x) = \frac{1}{c} \sum_{y \in N(x)} e^{\left(\frac{(X^2 - Y^2)}{2* \operatorname{sigma}_{d} d^2}\right)} e^{\left(\frac{-I(X^2 - Y^2)}{2* \operatorname{sigma}_{d} r^2}\right)}$$
(2)

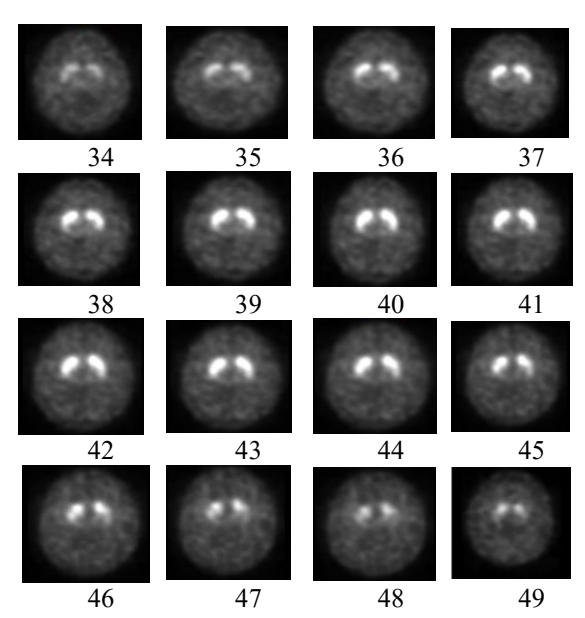


Figure 3: Selected slices of rich striatal uptake image slices

The weights corresponding to the spatial and intensity domains are represented by the parameters 'sigma_r' and 'sigma_d', respectively, in the equation. N(x) represents the spatial relationship between adjacent pixels in the image, and a constant "C" is also utilized for normalization. The formula for this normalization constant, 'C' could be

$$C = \sum_{y \in N(x)} e^{\left(\frac{(X^2 - Y^2)}{2* \text{sigma}} d^2\right)} e^{\left(\frac{-I(X^2 - Y^2)}{2* \text{sigma} r^2}\right)}$$
(3)

This equation has been effectively employed to achieve consistent and well-defined edges in the image, as it helps in reducing noise [22]. The goal here is to isolate regions of high intensity from the surrounding areas in the image, particularly focusing on segmenting the striatum from the background based on intensity. To achieve this, a straightforward segmentation method is applied, known as thresholding. This technique simplifies the process of extracting the region with high striatal uptake while minimizing the impact of noise outside this region. The DaT (Dopamine Transporter) content within the striatum exhibits a gradient from lower intensity in the putamen to higher intensity in the caudate within the VCDIS. Therefore, VCDIS are employed with a specific threshold value (separate value for EPD and HI) to accurately segment the image. The region of interest is represented as '1,' while the remainder of the image is marked as '0,' according to the binary representation produced by this segmentation [19].

2.4 Feature extraction

The primary objective of feature extraction is to obtain quantitative information for distinguishing HI from EPD cases. The link between grayscale levels in an image and the striatum's morphology changes results change of dopamine levels within the striatum. The shape is changed from a "comma" to a "dot" by this transition.

Consequently, the texture and shape characteristics are proven to be effective discriminators between the anatomical structures of HI and EPD. To achieve this discrimination, various features, including mean, area, entropy, correlation, and sharpness estimation are computed from the VCDIS [19, 21, 22]. These features are derived from the binary images and are quantified using the equations provided in Table 1

2.5 The Concept of DNFS

Table 1: The detailed description of the shape and texture features used

Features	Formula
Mean	$\mu\overline{(i,j)} = \frac{\sum (i,j)}{N}$ $\underline{\sum (i,j)_{p_{i,j}} - \mu^2}$
Correlation	$\frac{\sum (i,j)_{p_{i,j}} - \mu^2}{\sigma^2}$
Entropy	-sum (p *log2 (p))
Area	$A = \sum P_{i,j}$
Sharpness Estimation	$\sqrt{S_x^2 - S_y^2}$, Sx- The ratio of distinct (sharp) pixels to pixels found at the edges.
SBR	(Pu_L+ Ca_L+Pu_R+Ca_R / occipital region) – 1

Where, p – Probability of the gray level, N - pixels' number, σ - standard deviation, μ - mean value

Deep Neuro-Fuzzy Systems (DNFS) represent a better version of the Adaptive Neuro-Fuzzy Inference System (ANFIS) and the Deep Neuro-Fuzzy Inference System (DNFIS). DNFS integrates the learning capabilities of artificial neural networks with the interpretability and reasoning power of fuzzy logic, forming a hybrid system adept at handling time-varying, dynamic, and nonstationary data more effectively [23]. As an advanced hybrid Artificial Intelligence (AI) model, DNFS combines Fuzzy Logic (FL) with Deep Learning (DL) across multiple stages to address complex classification tasks in the diagnosis of EPD. This integration allows the system to extract and utilize deep, high-level features from various forms of medical data while preserving the semantic transparency and rule-based structure of fuzzy systems [24].

In the context of PD diagnosis, DNFS operates using nine input features like mean, entropy, correlation, sharpness estimation, area, and SBR values from left and right putamen (Pu_L, Pu_R) and caudate (Ca_L, Ca_R). The system yields a single binary output indicating whether the person is suffering from PD or not. The dynamic nature of DNFS enables it to adaptively frame its system structure in response to the characteristics of the input dataset. This adaptability contributes to enhanced diagnostic performance, particularly in identifying EPD, where subtle and non-linear patterns may otherwise be difficult to detect using conventional models.

The key conceptual structure of DNFS is stated below.

2.5.1 **Input layer:**

The input layer combines shape, texture features like mean, entropy, correlation, area, sharpness estimation and the SBR values. Hence, it is named as multimodal dataset which is given to Convolutional Neural Network (CNN) for capturing hidden relationships between the features.

2.5.2 **Feature Selection using CNN:**

CNN is incorporated here to learn and select meaningful temporal and spatial correlations of the features automatically. It also eradicates noises present in the data. CNN uses two stages of Convolutional layer of filter size 32 and 64, kernel size 3 and the activation function RELU is chosen in such a way that it selects most prominent features from the dataset. A max pooling layer with a pool size of 2 is used to reduce spatial dimensions and eliminate redundant information, while a dropout layer is employed to prevent overfitting by randomly deactivating neurons during training. The sigmoidal activation function is final layer of DNFS that is utilized to convert the features into non-linear representations or classifying the features.

2.5.3 **Fuzzification or Fuzzy Layer:**

This layer plays an important role in interpreting the input dataset. It maps the shape, texture features and SBR values into fuzzy linguistic terms (e.g. low, medium and high) makes human-understandable and decisions diagnosing EPD. The Gaussian membership function (GMF) is used for providing a smooth transition between membership degrees. The mathematical expression of GMF is given as

$$\mu(x) = e^{-\frac{(x-c)^2}{2\sigma^2}} \tag{4}$$

Where x, c, σ denote input value, mean value and standard deviation of the inputs respectively

2.5.4 **Rules sets:**

DNFS uses data to create "if-then" fuzzy rules with the help of FS. These rules verbally express the connections between certain features (mean, area, and SBR values of Pu_L, Pu_R, Ca_L, and Ca_R) and outputs (whether or not the person has PD). FS frames sample rules as:

IF Area is x₁and Mean is x₂ and Ca_L is x₃ and Ca_R is (a) (b) Rule Optimization using PSO x4 and Pu_L is x5 and Pu_R is x6 THEN $q = o_1$ IF Area is y₁ and Mean is y₂ and Ca_L is y₃ and Ca_R is y4 and Pu_L is y5 and Pu_R is y6, THEN $q = o_2$ where x_1, x_2, \dots and $y_1, y_2 \dots$ are fuzzy sets and o_1, o_2, \dots are constants [25].

The algorithms GA and PSO are used to optimize the fuzzy rule sets for accurate calculation of the EPD by minimizing classification errors, redundant and conflicting rules. In order to improve the rules' interpretability, classification accuracy, and redundancy, the fuzzy rule layer of DNFS uses PSO and GA. These algorithms ensure that the generated rules are the most effective in distinguishing EPD from HI. The conceptual procedure of both the algorithms is given below.

(a) Procedure for Genetic Algorithm

The GA follows an evolutionary approach to refine fuzzy rules in DNFS workflow. The procedure begins with an initial population of arbitrarily made rule sets that are assessed using a fitness function. The selection method picks the most optimized rule sets, which then undergo crossover to generate combinations of new fuzzy rule, preserving crucial forms among the features. In addition, mutation is utilized to prevent the algorithm being stuck with local optima. This iterative process continues until a maximum convergence is met. By optimizing fuzzy rules and membership functions, GA enhances decision-making in DNFS, leading to more exact and reliable PD diagnosis. The Conceptual procedure portrays in Figure 4.



Repeat steps 2-5 until the rules stabilize Figure 4: Conceptual procedure for GA

PSO is employed for optimizing fuzzy rules to enhance classification accuracy of EPD diagnosis. It is a population-based algorithm that draws inspiration from fish and bird swarm intelligence. The work flow of PSO is depicted in Table.2

Table 2: The overall work flow of PSO

Table 2: The overall work flow of PSO					
Step 1	Initialize the Swarm				
Step 2	Evaluate Fitness of Each Rule				
Step 3	Identify Best Rules				
Step 4	Update Velocity & Position of Rules by				
	adjusting rule parameters				
Step 5	Update Rules & Repeat				
Step 6	Select Optimized Rules [26]				

2.5.5 Aggregation and Defuzzification Layer

Each fuzzy rule generates a fuzzy set based on the selected features. The aggregation layer combines multiple fuzzy sets to generate a final fuzzy output. The Weighted Average Aggregation (WAA) method is applied in diagnosing EPD due to its capability of considering the strength of all rules and handling the noise, uncertainty of the dataset. WAA computes a weighted sum of all the fuzzy rule and its mathematical equation is given as

$$\sigma_{agg} = \frac{\sum (\sigma_i \cdot \omega_i)}{\sum \omega_i} \tag{5}$$

where σ_i and ω_i denotes membership value and weightage of the fuzzy rule.

The aggregated fuzzy output is transformed into a clear number value by the final defuzzification layer, indicating whether or not the patient has EPD. It provides the output with the help of Centre of Gravity (CoG) that produces the most stable and accurate diagnosis by handling overlapping fuzzy sets well. The CoG is expressed as

$$z = \frac{\sum \sigma(y).y_i}{\sum \sigma(y)} \tag{6}$$

0.7

1000

where $\sigma(y)$ and y_i denotes membership value, and discrete output value.

Table 3: Parameters of particle swarm optimization (PSO)and genetic algorithm (GA)

Parameter	Typical Value					
	range					
Genetic Algorithm						
Population Size	20					
Mutation Rate	0.2					
Crossover Rate	0.7					
Selection Method	Tournament					
	Selection, size $=3$					
Number of Generations	1000					
Particle Swarm Optimization						
Swarm Size	20					
Inertia Weight (w)	0.5					
Cognitive Coefficient (c1)	1.5					
Social Coefficient (c2)	1.5					

To determine whether the patient has the disease or not, the threshold value (0.5) is applied to the defuzzification output. To make generalization between the chosen features and a single output, the DNFS classification model's workflow adjusts the GMF's hyperparameter. The training and testing datasets are separated into 70:30 and 80:20 sections.

Velocity Limits (Vmax)

Number of Iterations

With the stopping condition set at 1000, the hyperparameters of optimization algorithms like GA and PSO are selected based on refined through empirical testing to ensure stable convergence and high classification accuracy as shown in table 3. And the Table 4 provides the pseudo code for the DNFS classification process.

Table 4: Training procedure for DNFS

- Load VCDIS and extract the features like shape, texture and SBR values.
- 2. Frame DNFS classification model
 - a. Select the prominent features using CNN
 - b. Define membership function to the features
 - c. Frame rules automatically using FS for features
 - d. Optimize the rules using GA/PSO.
 - e. Aggregate the fuzzy rules and perform defuzzification
 - f. Estimate the performance indicators (Loss, Accuracy, F1-Score, Recall, Precision)
 - g. Classify effectively EPD from HI

3 Results and discussions

3.1 Image processing

The bilateral filter, which preprocesses the VCDIS, evaluates performance using sigma_d (spatial) and sigma_r (intensity) as the two parameters. To identify the ideal filter parameter values, an analysis [27] is carried out. According to this research, sigma_d is between 1.5 and 2.0. In this study, image edges are preserved by using a value of 1.5. However, a lesser number, such as 0.1, is selected because sigma_r changes greatly with noise levels. For the processed image to be accurate, the parameter values are essential. The processed (filtered) VCDIS for both HI and Early PD are shown in Figure 5(ii) and (v), which show variations in dopamine transporters. In EPD, the content of the dopamine appears decreased to be like a dot or like a circular within one side of the striatum, but in HI, it appears comma-shaped.

Initially, in EPD, the content of dopamine is notably absent in the putamen, corresponding to regions with low intensity values. Subsequently, the caudate also experiences a loss of DaT content. The suggested approach uses a thresholding technique to segregate these high-intensity regions, starting from the left side of the striatum and working its way to the right. To ensure objectivity in the segmentation process, a normalizing process is done before thresholding [28]. The average and standard deviation (SD) of the threshold values is determined to be 2.1e4±0.5 for EPD and 1.8e4±0.7 for HI after careful assessment. The VCDIS histogram values are used as the basis for selecting these threshold values. The segmented images, shown in Figure 5 (iii) and (vi), exhibit a substantial distinction between EPD and HI when compared to prior research [13]

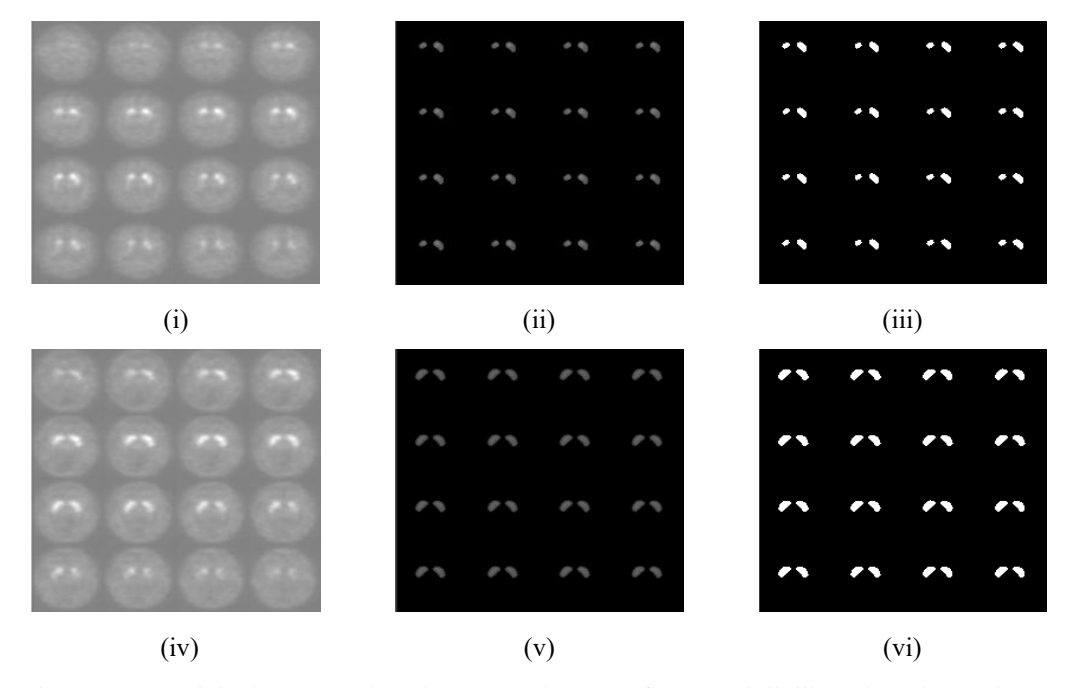


Figure 5: The original, processed, and segmented VCDIS for EPD (i, ii, iii) and HI (iv, v, vi)

Table 5: Average and SD values of the features

Features	EP	D	Н		
reatures	Average	SD	Average	SD	p level
Area	240.000	70.440	385.689	30.854	0.01
Mean	466.257	51.508	688.136	12.885	0.00
Correlation	0.542	0.082	0.682	0.055	0.03
Entropy	0.174	0.082	0.195	0.031	0.02
Sharpness Estimation	12.828	5.766	15.182	1.811	0.00
Ca_R	1.984	0.611	2.933	0.604	0.03
Ca_L	1.994	0.600	2.967	0.618	0.03
Pu_R	0.856	0.397	2.119	0.582	0.01
Pu_L	0.822	0.375	2.116	0.573	0.02

p denotes the significant level of EPD and HI(p<0.05).

3.2 Extraction of feature

It is clear that EPD is typified by a decrease in DaT content, which causes the striatum-more especially, the putamen and caudate regions—to shrink. As the DaT content decreases, the natural shape, which resembles a comma, changes to a smaller, dot-like or circular look in transformation enables EPD. This quantitative measurement of the striatal areas. The VCDIS texture features show how the gray levels interact. Shape and texture extracted features include mean, area, correlation, entropy, and sharpness estimation. SBR values are also included to improve classifier performance. Table 5 shows the average and SD values of features for HI and EPD. The table highlights important deviations between HI and EPD features, suggesting higher performance in accurate classification and easier processing, which is confirmed by the p-value of HI and EPD, which is less than 0.05 and falls within a 5% acceptance level.

The striatal area (comprising putamen and caudate) is notably smaller in EPD compared to HI, measuring 240.000 and 385.689 respectively. These measurements underscore substantial changes in EPD. Features that show higher values in HI but lower values in EPD include mean, area, entropy, and correlation. This indicates significant differences between features linked to shape and texture, which eventually improves classification accuracy.

Features	Low	Medium	High
Area	126.38 to 200.12	202.36 to 299.37	300.75 to 661.31
Mean	183.75 to 349.50	350.12 to 448.75	450.00 to 661.37
Ca_L	0.51 to 2.28	2.29 to 3.42	3.43 to 4.61
Ca_R	0.36 to 2.00	2.01 to 3.00	3.01 to 4.96
Pu_L	0.34 to 1.97	1.98 to 2.49	2.50 to 3.52
Pu_R	0.29 to 1.09	1.10 to 2.06	2.07 to 2.99

Table 6: The Linguistic terms and its values of selected features

3.3 Performance of DNFS framework with optimized algorithms

DNFS procedure starts with selecting the most prominent features using simple two stage CNN model. The model learns non-linear relationships among the data and selects the most optimized features such as Area, Mean, Ca_L, Ca_R, Pu_L and Pu_R. These selected features are utilized further for diagnosing EPD. These features are not varying sharply; but gradually. Hence, these gradual transitions are captured by GMF and gives the realistic or linguistic terms like low, medium and high as given in Table.6

Table 7: The fuzzy rule for diagnosing early stage PD IF Area is Low **AND** Pu_L is Low **AND** Pu_R is Low **THEN** it is Early PD.

IF Ca_L is High **AND** Ca_R is High **AND** Pu_L is Medium **AND** Pu_R is Medium **THEN** it is HI

IF Mean is Low **AND** Pu_L is Low **THEN** it is Early PD IF Ca_L is Low **AND** Ca_R is Low **AND** Mean is Low **THEN** it is Early PD

IF Area is High **AND** Mean is High **AND** Ca_L is High **AND** Ca_R is High **THEN** it is Normal

The linguistic terms like low, medium and high values of the features are utilized for framing fuzzy rules using GMF. The average number of fuzzy rules framed are 18.2±2.3. Some of the fuzzy rules are given in Table. 7. These rules are optimized using GA and PSO.

The DNFS-PSO and DNFS-GA models are created and run separately to predict EPD. The redundant rules removed from the rule sets are 12.6%, 7.4% for DNFS-PSO and DNFS-GA respectively. 70% and 80% of the data are utilized for training the models with 1000 iterations, and the remaining portion is used for testing. Table 8 displays the average (Mean) performance metrics over 1000 iterations of the developed DNFS-PSO and DNFS-GA for various learning rates of 0.001, 0.01, and 0.1 in terms of accuracy, loss, F1 score, precision, and recall. A detailed look at table 8 shows that the best model for EPD prediction is DNFS-PSO, with accuracy, F1-

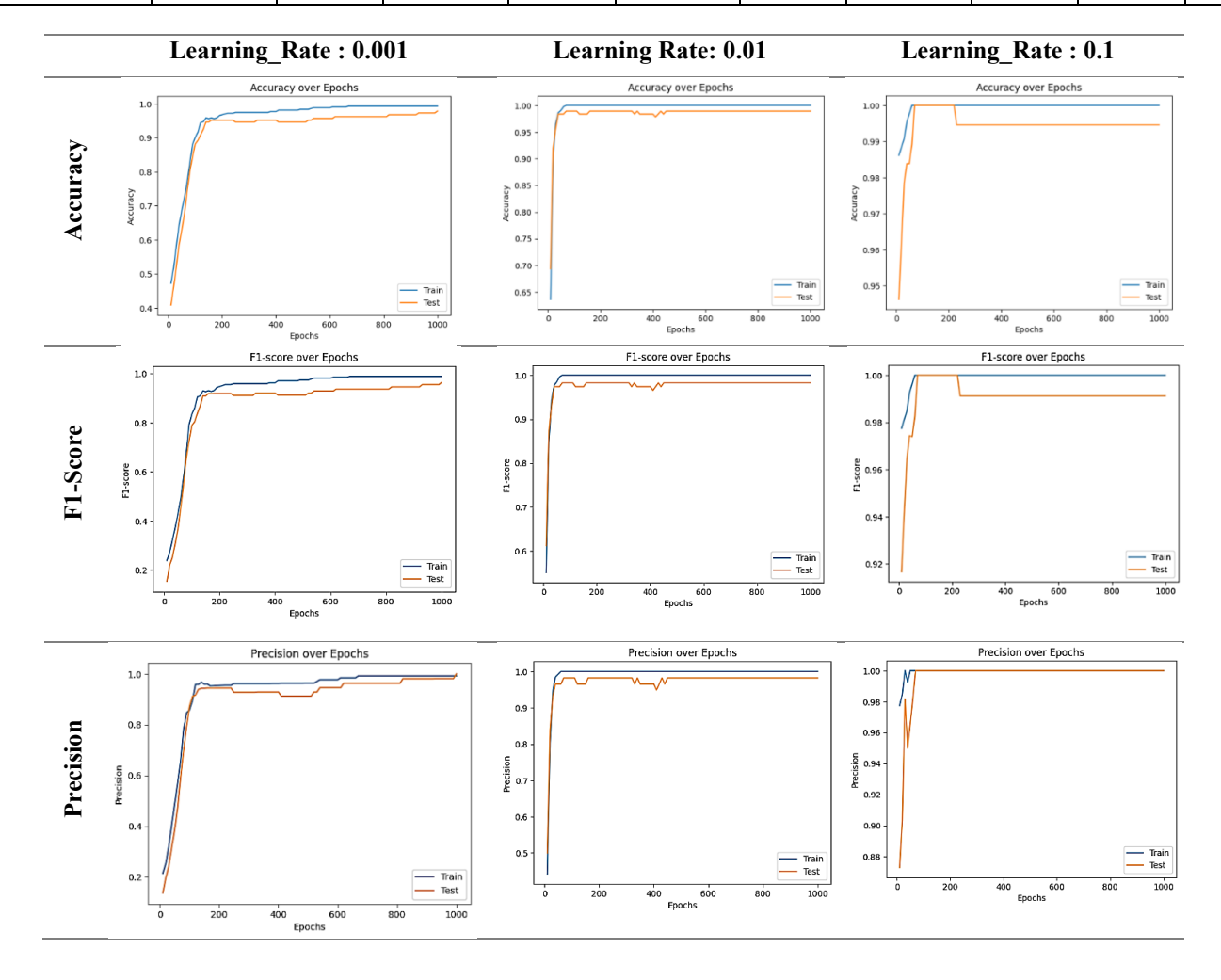
score, precision, and recall values (Mean±SD) of 98.77±1.02%, 0.99±0.12, 1.0±0.01, and 0.99±0.10 for the splitting ratio of 70:30 and learning rate of 0.01 respectively. With a splitting ratio of 70:30 and a learning rate of 0.01 for detecting EPD, DNFS with PSO provides the best results in terms of loss, accuracy, precision, recall, and F1-score. Figure 6 and 7 shows the performance graph (1000 iterations) of two optimization algorithms, DNFS-GA and DNFS-PSO models, for learning rates 0.001, 0.01, and 0.1 for 70:30 and 80:20.

With a loss of 0.0199, the DNFS-PSO model offers the lowest. According to the performance metrics, the suggested DNFS augmented with PSO is more effective than DNFS-GA at diagnosing PD. The model accurately predicts the negative (HI) and positive (EPD) cases in categorizing HI and EPD, as indicated by the precision and recall values of 1.0±0.01, and 0.99±0.10 respectively. When the learning rate is 0.01 the model does well. An excessively high learning rate (0.1) can cause uncertainty, whereas 0.001 is too small causes sluggish convergence. Therefore, in the proposed study, the learning rate is set at 0.01 based on empirical method. The table demonstrates both DNFS-PSO and DNFS-GA achieved commendable diagnostic accuracy. Additionally, the statistical significance of both frameworks is confirmed, as the p-values for p1 (70:30 split) and p2 (80:20 split) are below 0.05.

The system's performance is measured by comparing it to machine learning and optimization techniques and it displays the extreme level of accurate accuracy across all the networks, as demonstrated in Table 9. This new method's diagnostic accuracy is strongly linked to the earlier research. To minimize bias, variation, and overfitting, the suggested method uses 10000 iterations and an optimum methodology for selecting features, producing reliable and consistent results. For specialists in differentiating between EPD and HI, this method is easy to use and practical, and it eventually produces better results than the systems discovered in the literature. In addition, the proposed model offers best performance due its dynamic nature in framing rule sets and self-adapting model.

Table 8: The Averaged performance Results of DNFS-PSO and DNFS-GA

Evaluation	Splitting Ratio 70:30 Splitting Ratio 80:20									
Metrics	DNFS-GA DNF		DNFS	S-PSO DN		5-GA	DNFS	DNFS-PSO		P2
	Training	Testing	Training	Testing	Training	Testing	Training	Testing		
		•		Learnin	ng Rate: 0.001					
Loss	0.1769	0.1342	0.1897	0.1654	0.1897	0.1051	0.1887	0.1754	0.04	0.05
Accu. (%)	97.85	98.310	98.390	98.310	95.970	98.80	98.230	98.31	0.04	0.04
F1-Score	0.9636	0.9887	0.9735	0.9888	0.9315	0.9967	0.9735	0.9812	0.03	0.04
Precision	0.975	0.9924	0.9821	0.9851	0.9714	1.070	0.9721	0.9751	0.04	0.03
Recall	0.9298	0.9850	0.9649	0.9825	0.8947	0.9934	0.9630	0.9825	0.05	0.05
Learning Rate: 0.01										
Loss	0.2633	0.2444	0.0013	0.0199	0.0209	0.0536	0.0195	0.0019	0.03	0.02
Accu. (%)	94.93	97.32	99.92	98.77	99.80	98.11	99.14	97.99	0.01	0.03
F1-Score	0.9247	0.9524	0.9925	0.99	0.9967	0.9867	0.9825	0.9880	0.03	0.05
Precision	0.8824	0.9259	0.9831	1.0	0.9935	1.0	0.9831	0.9985	0.02	0.04
Recall	0.9712	0.9804	0.9825	0.99	1.0	0.9737	0.9825	1.0	0.04	0.02
Learning Rate: 0.1										
Loss	0.0116	0.0045	0.0034	0.0677	0.0885	0.0562	0.0287	0.0016	0.04	0.05
Accu. (%)	97.31	98.16	99.82	98.19	97.58	98.60	98.66	98.79	0.03	0.04
F1-Score	0.96	0.9892	0.9995	1.0	0.9565	0.9765	0.9895	0.999	0.04	0.03
Precision	1.0	0.9793	1.0	1.0	0.9706	0.9835	1.0	0.999	0.04	0.03
Recall	0.9231	0.9792	0.9925	1.0	0.9429	0.9642	0.9775	0.999	0.03	0.04



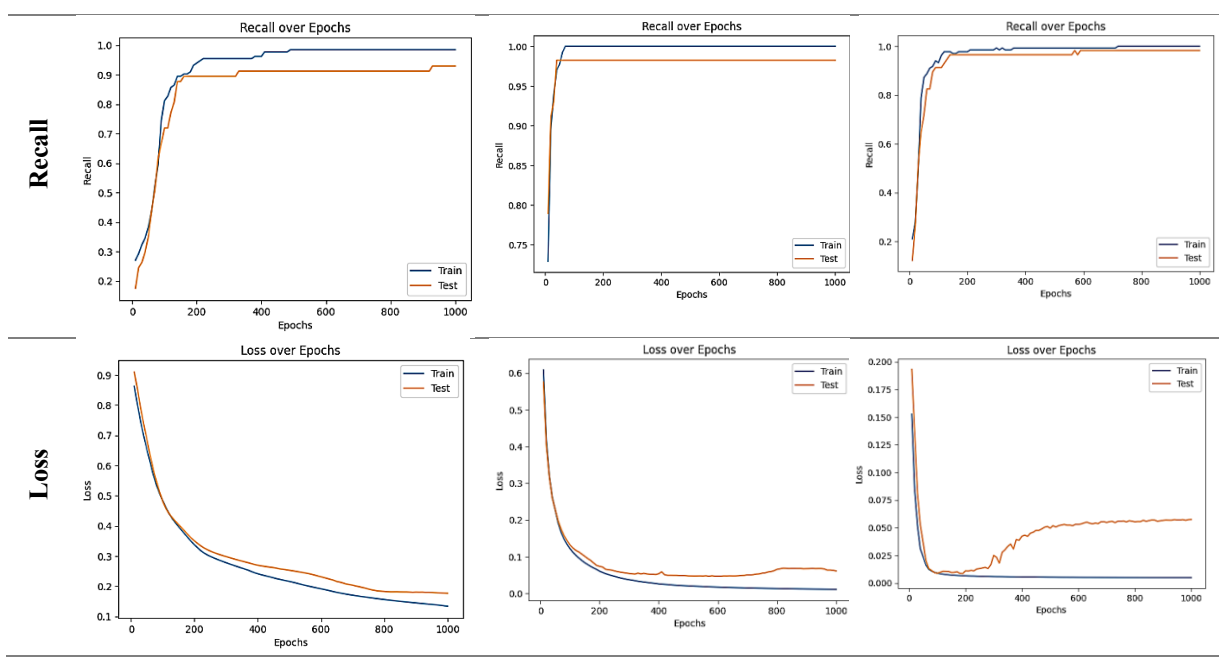
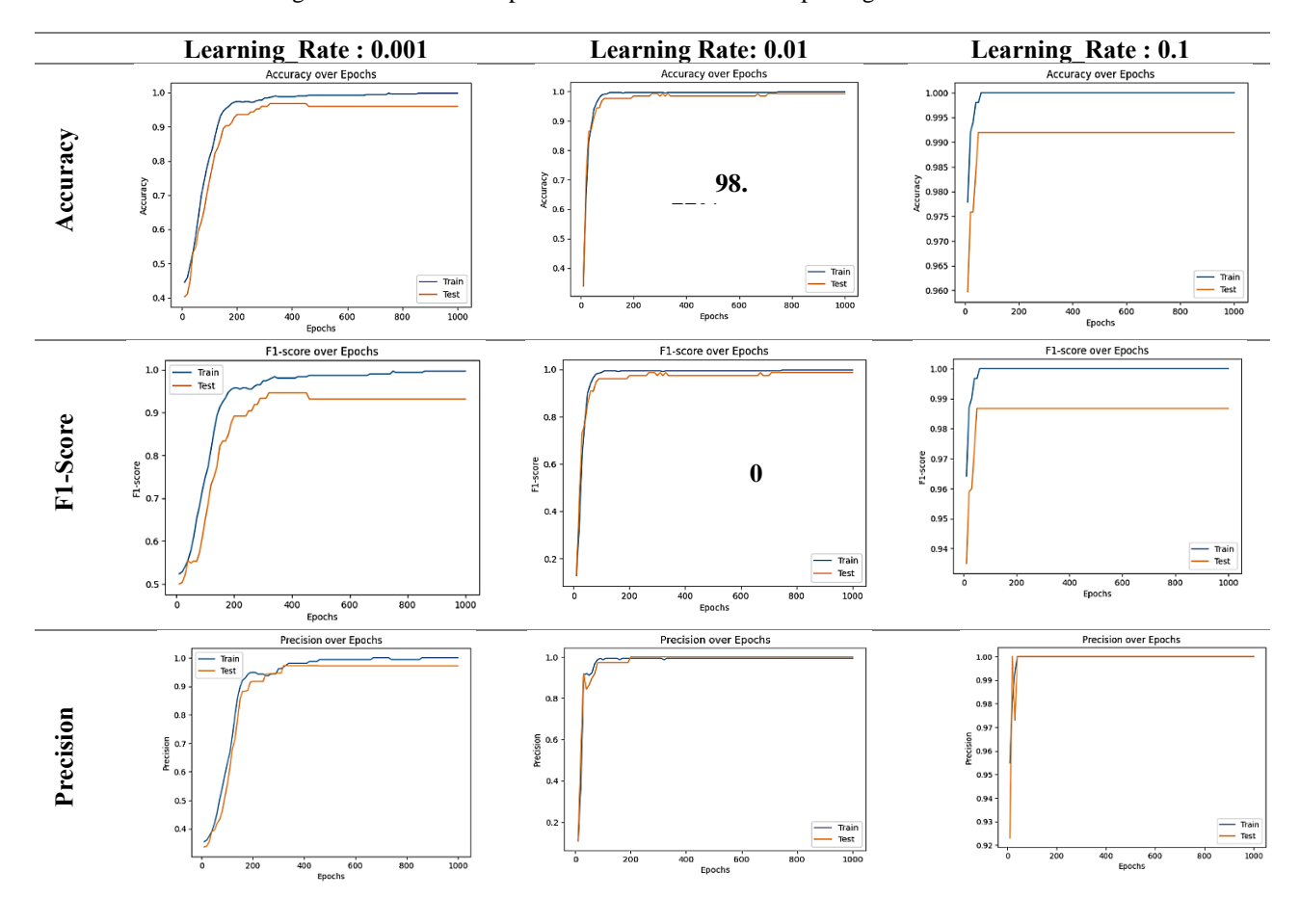


Figure 6: Performance plot for DNFS PSO for the splitting ratio of 80:20



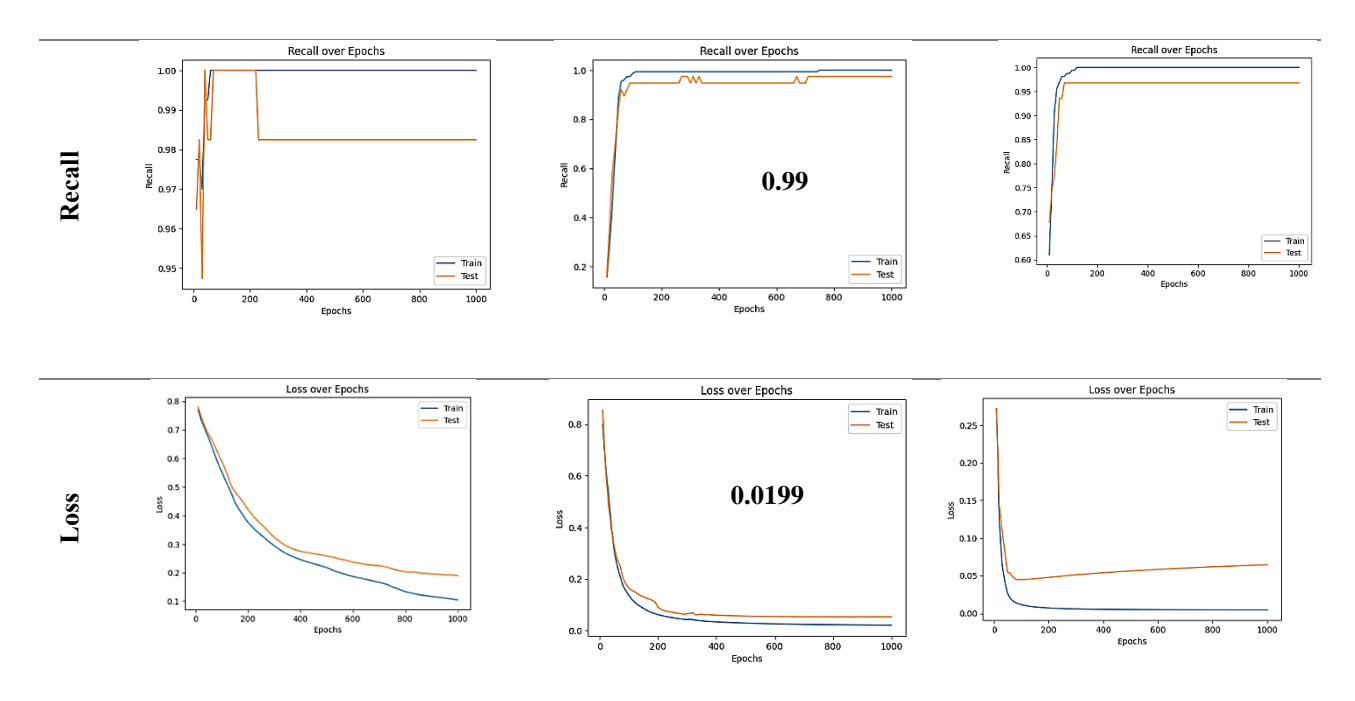


Figure 7: Performance plot for DNFS PSO for the splitting ratio of 70: 30

S. No.	Details	Methodology used	Performance (%)
1	Anita et al [13]	VRIS with RBF-ELM	98.23
2	El-Hasnony et al. [15]	Fog-based ANFIS+PSOGWO model	87.50
3	Balasubramanian K et al [16]	Modified glow worm swarm optimization algorithm (M-GSO)	95.00
4	Prashanth et al. [21]	Averaged single image slice with SVM	97.29
6	Proposed Work	DNFS -PSO	98.77

Table 9: Comparative analysis of the literature

4 Discussion

The proposed DNFS framework, optimized using PSO and GA, demonstrates high accuracy in detecting Early Parkinson's Disease (EPD) using VCDIS images. Bilateral filtering with $\sigma_{-} d = 1.5$ and $\sigma_{-} r = 0.1$ effectively reduces noise while preserving edge details. Thresholding and normalization techniques enable accurate segmentation of dopamine-rich regions, revealing clear morphological differences between EPD and HI, particularly in the putamen and caudate.

Feature extraction based on shape, texture, and SBR values highlights significant statistical differences (p < 0.05) between the two classes. A two-stage CNN selects key features, which are converted into linguistic terms using GMF and refined through fuzzy rule optimization via PSO and GA.

Among the models, DNFS-PSO achieves superior performance, with 98.77±1.02% accuracy, 0.99±0.12 F1-score, and minimal loss of 0.0199 at a learning rate of 0.01 and 70:30 data split. Performance graphs confirm the model's robustness and stability. The results validate the framework's effectiveness in early-stage PD detection and classification.

5 Conclusion

Parkinson's disease (PD) is a crippling neurological condition that significantly lowers a person's quality of life. The progressive loss of dopamine-producing neurons in the mid-region of the brain, which is the hallmark of PD, emphasizes the importance of early detection and treatment. To improve prediction accuracy and enable early intervention, researchers are always experimenting with different approaches and technology. A major breakthrough in the field of EPD diagnosis is represented by the novel prediction framework of the proposed study, which combines Deep Neuro-Fuzzy Systems (DNFS) with Particle Swarm Optimization (PSO) and Genetic Algorithm (GA). Using loss, accuracy, precision, recall, and F1-score as performance metrics, this model was thoroughly assessed using Volume Containing DaTscan Image Slices (VCDIS) from the Parkinson's Progression Markers Initiative (PPMI). With an impressive 98.77% classification accuracy and low error rates, the study's findings are incredibly encouraging. Crucially, this performance outperforms previously documented classification techniques in the body of current research, confirming the DNFS-PSO model's capacity to forecast Parkinson's disease in its early stages. This study represents a significant milestone in the quest to improve the early identification and management of Parkinson's Disease. In the future, a range of diverse techniques and optimizations will be employed to achieve superior performance

Statements and declarations

Funding: Not applicable.

Competing Interests: There are no conflicts of interest among the authors.

Author Contributions: All authors contributed to the study conception and design. Material preparation, data collection and analysis were performed by Jothi S, Anita S, and Sivakumar S. The first draft of the manuscript was written by Anita S and all authors commented on previous versions of the manuscript. All authors read and approved the final manuscript.

Ethical approval: The authors used de-identified public data and hence did not require IRB approval.

Availability of data and materials: https://www.ppmi-info.org/access-data-specimens/download-data

References

- [1] Konnova, E.A. and Swanberg, M., 2018. Animal models of Parkinson's disease. In: T.B. Stoker and J.C. Greenland, eds. Parkinson's Disease: Pathogenesis and Clinical Aspects [online]. Brisbane (AU): Codon Publications, Chapter 5. Available at: https://pubmed.ncbi.nlm.nih.gov/30702844
- [2] Mahmood, A., Khan, M.M., Imran, M., Alhajlah, O., Dhahri, H. and Karamat, T., 2023. End-to-end deep learning method for detection of invasive Parkinson's disease. Diagnostics, 13(6), p.1088. https://doi.org/10.3390/diagnostics13061088
- [3] Constantinides, V.C. et al., 2023. Dopamine transporter SPECT imaging in Parkinson's disease and atypical Parkinsonism: A study of 137 patients. Neurological Sciences, 44(5), pp.1613–1623. https://doi.org/10.1007/s10072-023-06628-9
- [4] Prashanth, R., Roy, S.D., Mandal, P. and Ghosh, S., 2014. Automatic classification and prediction models for early Parkinson's disease diagnosis from SPECT imaging. Expert Systems with Applications, 41, pp.3333–3342. https://doi.org/10.1016/j.eswa.2013.11.031
- [5] Kaufman, M.J. and Madras, B.K., 1991. Severe depletion of cocaine recognition sites associated with the dopamine transporter in Parkinson's-diseased striatum. Synapse, 9, pp.43–49. https://doi.org/10.1002/syn.890090107
- [6] Cummings, J.L. et al., 2011. The role of dopaminergic imaging in patients with symptoms of dopaminergic system neurodegeneration. Brain, 134, pp.3146–3166. https://doi.org/10.1093/brain/awr177
- [7] Moore, D.J., West, A.B., Dawson, V.L. and Dawson, T.M., 2005. Molecular pathophysiology of Parkinson's disease. Annual Review of Neuroscience, 28, pp.57–87. https://doi.org/10.1146/annurev.neuro.28.061604.13 5718

- [8] Booth, T.C. et al., 2015. The role of functional dopamine transporter. AJNR: American Journal of Neuroradiology, 36, pp.229–235. https://doi.org/10.3174/ajnr.A3970
- [9] Bairactaris, C. et al., 2009. Impact of dopamine transporter single photon emission computed tomography imaging using I-123 ioflupane on diagnoses of patients with Parkinsonian syndromes. Journal of Clinical Neuroscience, 16, pp.246–252. https://doi.org/10.1016/j.jocn.2008.01.020
- [10] Marek, K. et al., 2011. The Parkinson Progression Marker Initiative (PPMI). Progress in Neurobiology, 95, pp.629–635. https://doi.org/10.1016/j.pneurobio.2011.09.005
- [11] Prashanth, R., Roy, S.D., Ghosh, S. and Mandal, K.P., 2013. Shape features as biomarkers in early Parkinson's disease. In: 6th International IEEE/EMBS Conference on Neural Engineering (NER). https://doi.org/10.1109/NER.2013.6695985
- [12] Susanna Jakobson, Jan Linder, Lars Forsgren, Katrine Riklund, "Accuracy of Visual Assessment of Dopamine Transporter Imaging in Early Parkinsonism", Movement disorder, Vol. 2 (1), March 2015, Pages 17-23, https://doi.org/10.1002/mdc3.12089
- [13] Anita, S. and Aruna Priya, P., 2020. Diagnosis of Parkinson's disease at an early stage using volume rendering SPECT image slices. Arabian Journal for Science and Engineering, 45, pp.2799–2811. https://doi.org/10.1007/s13369-019-04152-7
- [14] Talpur, N. et al., 2022. A comprehensive review of deep neuro-fuzzy system architectures and their optimization methods. Neural Computing and Applications, 34(6), pp.1–39. https://doi.org/10.1007/s00521-021-06807-9
- [15] Rana, J., Raidah, S.A.L. and Khudeyer, S.A., 2024. Review: Deep learning and fuzzy logic applications. Engineering and Technology Journal, 9(6), pp.4231–4240. https://doi.org/10.47191/etj/v9i06.09
- [16] Talpur, N., Abdulkadir, S.J., Alhussian, H. et al. Deep Neuro-Fuzzy System application trends, challenges, and future perspectives: a systematic survey. Artif Intell Rev 56, 865–913 (2023). https://doi.org/10.1007/s10462-022-10188-3
- [17] Bo Wang, A Hybrid Fuzzy Logic and Deep Learning Model for Corpus-Based German Language Learning with NLP. Informatica, Informatica 49 (2025) 1–14. https://doi.org/10.31449/inf.v49i21.7423
- [18] Aversano, L., Bernardi, M.L., Cimitile, M. and Pecori, R., 2020. Fuzzy neural networks to detect Parkinson disease. In: IEEE International Conference on Fuzzy Systems, pp.1–8. https://doi.org/10.1109/FUZZ48607.2020.9177948
- [19] Masood, S., Sharif, M., Masood, A. et al., 2015. A survey on medical image segmentation. Current Medical Imaging Reviews, 11(1), pp.3–14. https://doi.org/10.2174/15734056110115042310344
- [20] Djang, D.S. et al., 2012. SNM practice guideline for dopamine transporter imaging with 123I-ioflupane

- SPECT 1.0. Journal of Nuclear Medicine, 53, pp.154–163. https://doi.org/10.2967/jnumed.111.100784
- [21] Prashanth, R., 2015. Computer-aided early detection
- of Parkinson's disease through multimodal data analysis. Ph.D. thesis, Indian Institute Technology, Delhi.
- [22] Zhang, M., 2009. Bilateral filter in image processing. Master's Thesis, Louisiana State University.
- [23] Yang, C.H., Moi, S.H., Hou, M.F., Chuang, L.Y. and Lin, Y.D., 2020. Applications of deep learning and fuzzy systems to detect cancer mortality in nextgeneration genomic data. IEEE Transactions on **Fuzzy** Systems, pp.3833-3844. 29(12), https://doi.org/10.1109/TFUZZ.2020.3028909
- [24] Unal, Z. and Cetin, E.I., 2022. Fuzzy logic and deep learning integration in Likert type data. Afyon Kocatepe University Journal of Sciences and pp.112-125. Engineering, 22(1),https://doi.org/10.35414/akufemubid.1019671

- [25] Abiyev, R.H. and Abizade, S., 2016. Diagnosing Parkinson's diseases using fuzzy neural system. Computational and Mathematical Methods in Medicine, 2016, Article ID 1267919, 9 pages. https://doi.org/10.1155/2016/1267919
- Balasubramanian, K. and Ananthamoorthy, N.P., 2021. Improved adaptive neuro-fuzzy inference system based on modified glowworm swarm and differential evolution optimization algorithm for medical diagnosis. Neural Computing and pp.7649-7660. Applications, 33(13), https://doi.org/10.1007/s00521-020-05507-0
- [27] Georgiadis, P. et al., 2008. Computer aided discrimination between primary and secondary brain tumors on MRI: From 2D to 3D texture analysis. E-Journal of Science and Technology, 8, pp.9–18.
- [28] Sharma, N. et al., 2008. Segmentation and classification of medical images using textureprimitive features: Application of BAM-type artificial neural network. Journal of Medical Physics, pp.119–126. https://doi.org/10.4103/0971-6203.42763